Al-Furat Journal of Innovations in Mechanical and Sustainable Energy Engineering (FJIMSE)

Heat Pipe and Thermosyphon: A Review of Performance and Applications

Zahraa Hassan Imran[1] , Rana Ali Hussein[2]

(Al-Mussaib Technical College, Power Mechanic Engineering Technical Department, Iraq). E-mail: zahraa.hassan.tcm46@student.atu.edu.iq
(Al-Mussaib Technical College, Power Mechanic Engineering Technical Department, Iraq). E-mail: ranaa.h.78@atu.edu.iq
*Corresponding author E-mail: zahraa.hassan.tcm46@student.atu.edu.iq

Abstract. *A technology has developed rapidly in the recent industrial revolution, and many engineering disciplines have witnessed an emerging trend of efficient, reliable, and energy-saving thermal management systems. Therefore, it is no wonder that heat pipe technologies, including thermosyphon-based systems, have gained more popularity as passive thermal management technologies that can be easily designed and utilized. The purpose of this review paper is to present an overview of the different approaches to enhance the thermal performance of heat pipes and thermosyphon, present the operational limitations of the aforementioned technologies, and examine the behaviour of two-phase systems as discussed in the literature. Additionally, the impact of critical parameters, including the selection of geometry, filling ratio, working fluids and operating orientation, is emphasized as discussed in the literature. There is a lot of emphasis placed on thermosyphon applications in different disciplines of engineering, which is an indication of the importance of thermosyphon technologies in the real world. Therefore, based on the findings of the review, the current research aims to examine the loop thermosyphon system theoretically and experimentally, with emphasis on enhancing the condenser section of the thermosyphon system.*

Keywords: Thermosyphon; Heat pipe; Phase change Flow; Close loop thermosyphon.

1. INTRODUCTION

In many engineering fields, the process of generating heat and the cooling systems is very significant. This helps in the efficient management of thermal load, efficient energy conversion, efficient operation, and safe operation. This process is very significant in many fields, including the power generation industry, aircraft, automobile, and electronic industries, where the efficient management of heat is very crucial for the efficient operation of the systems. Engineers strive to create and install efficient cooling systems that improve energy efficiency while reducing their negative effects on the environment. Thus, the production of heat and cooling because they allow for optimal performance, durability, and safety, systems are essential to the success of engineering applications. Excess heat is created during many engineering processes and must be dissipated, particularly in situations involving microelectronic devices. One efficient way to move or dissipate heat is by using a heat pipe[1].

Heat pipes are passive thermal devices that rely on the phase change of a working fluid, typically alcohol or water, within a closed system that makes it easier for its function to transport heat from a high-temperature source to a low-temperature sink. Working fluid is related to the filling ratio, which is defined as the ratio of the volume of the charged liquid to the total volume of the heat pipe [2] [3] [4].

Heat pipes are broadly classified into two types: wicked heat pipes, which contain a porous wick that returns the working fluid by capillary action as shown in figure (1), and wickless devices

(thermosyphons), which rely on gravity and perform best with the condenser above the evaporator (vertical or small tilt angles) [5].

Wicked heat pipes can have several types of wicks, like sintered powder wicks[6], screen-mesh wicks [7], grooved wicks[8], or composite wicks[9], The main wick types are illustrated in figure (2). Heat pipes can also be further categorized according to their design and working mechanism, including flat heat pipes [10], U-Shape heat pipes [11], pulsating heat pipes [12], Rotating heat Pipe [13], and Micro heat Pipe [14] [15].

Abdali j k and Alwan A A, (2020) developed a theoretical and numerical model to study the phase-change phenomenon inside a finned wick heat pipe using distilled water as the working fluid. The researcher used an explicit technique to imitate the processes of evaporation and condensation to predict the temperature variation with time and position. The phase-change zone appeared around z = 35 cm in the evaporator and about z = 45 cm in the condenser. Cooling fins were installed in the condenser section to improve heat removal and improve the overall thermal distribution along the pipe. Figure (3) shown Schematic of the heat pipe [16].

Bhadra and Nookaraju, (2020) Investigated a copper heat pipe with a composite wick charged with ethanol by testing it under heating inputs ranging from 50 to 400 W. Temperature readings at the evaporator and condenser were collected while the condenser was cooled by water flowing at about 0.01 kg/s, with the pipe set at a 15° inclination. The heat transfer improved as the input power increased, but performance dropped at higher loads due to excessive vapor formation. A CFD model developed in ANSYS closely matched the experimental measurements, confirming the validity of the numerical approach for this composite-wick heat pipe [17].

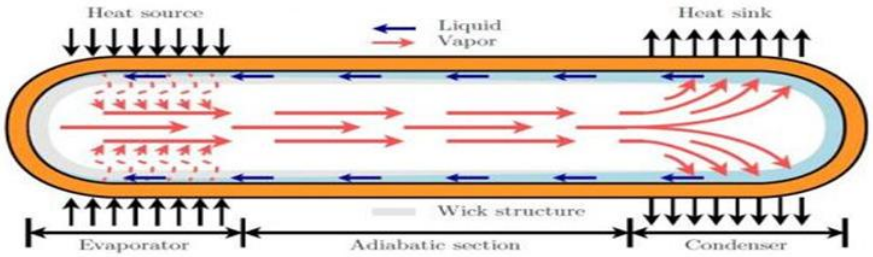

Fig. 1. A sketch of wicked heat pipes[18].

Fig. 2. Structures of wick [19].

2. THERMAL PERFORMANCE ENHANCEMENT

Researchers did not depend on adequate thermal performance of heat pipes and proceeded to introduce several methods for improving thermal performance. The main goal of thermal performance enhancement is to improve heat transmission. The graphic (3) shows a list of different methods [20]. In order to improve heat transfer by increasing the heat-exchanging surfaces, one among the most popular techniques in theoretical study and engineering use is the extended surface provided by fins. Fins have found use in heat exchangers with latent heat energy storage, condensation, thermoelectric cooling, nanofluid, and other types of applications [21]. Fin is basically classified into many types such as Annular fins[22], Longitudinal fins[23], Pin fin[24], helical fins[25], cylindrical fins [26],circular, square, and hexagonal fin [27] , and many other types.

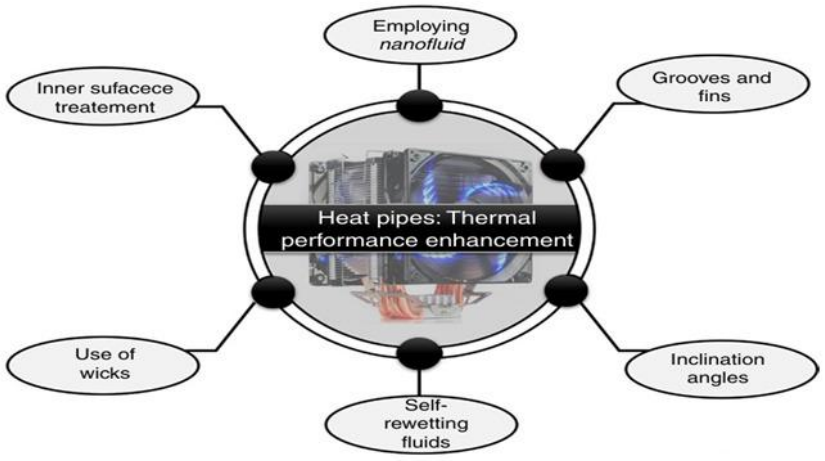

Fig. 3. Heat pipes: Thermal performance enhancement[20].

Fig. 4. A selection of available fin configurations[28].

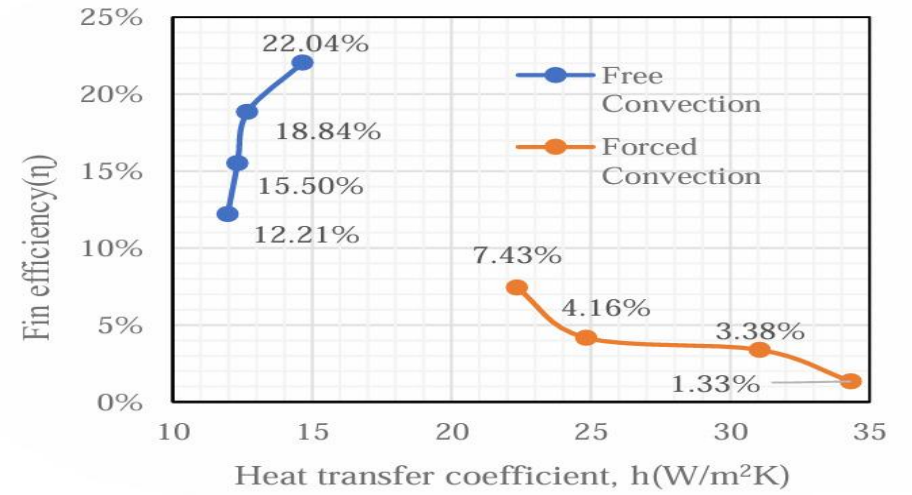

Fig. 5. Fin efficiency against Heat transfer coefficient[29].

Ahmed et al. (2020) conducted an experimental investigation on heat pipes integrated with helical fins to improve heat transfer efficiency. Two fin configurations featuring distinct helical pitches (20 mm and 40 mm) were evaluated under actual operational conditions in evacuated-tube solar collector including paraffin wax as a way to store thermal energy. The results showed that the narrower fin pitch (20 mm) worked better, with a maximum efficiency of 68.66% and an outlet fluid temperature of about 53°C at the lowest flow rate. Using fins and PCM also delayed the start of solidification by more than 1.5 hours after sunset, which kept the system's heat available for longer. The research showed that lowering the fin pitch does improve heat transmission and make heat-pipe-based thermal systems more efficient every day [30].

Tawsif Islam et al. (2023) Developed a copper closed-loop thermosyphon using analytical thermal calculations combined with MATLAB modelling to determine 15 fins, a fin efficiency of 0.82, an overall coefficient of heat transfer of 642.6 W/m²·°C, and a theoretical flow rate of 2.84 g/s. They then fabricated and tested the system using a 12.7-mm tube, water as the working fluid, and a 30-CFM cooling fan. The experiments demonstrated a heat-removal capacity of about 107 W and an overall cooler efficiency of 71.3%. The MATLAB predictions closely aligned with the measured thermal performance; Figure 16 shows the change in the number of fins based on the material used [31].

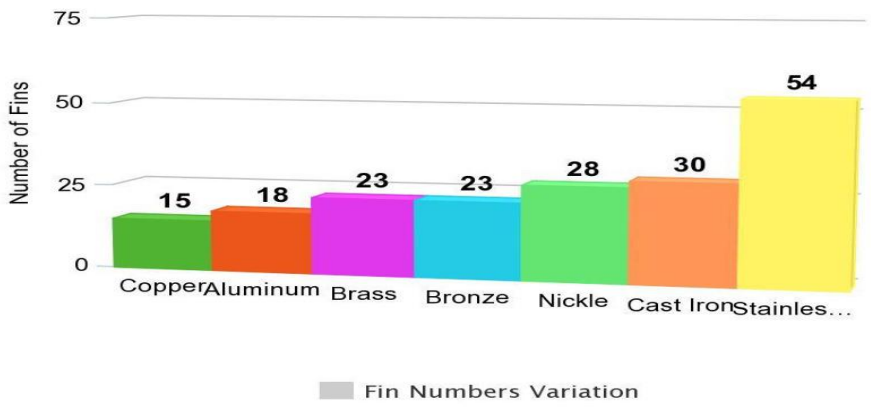

Fig. 6. Fin number variation [31].

ATU- FJIMSE, Vol. 4 No. 1 (2026): volume 4,Issu 1,May 2026 , All Rights Reserved

Tan et al. (2024) has created a copper loop thermosyphon of dimensions 135x650mm with an internally finned condenser to improve heat transfer, as seen in Figure (14). The test was performed with pure water and a suspension of microencapsulated PCM with 6 µm diameter and a melting point of 70°C. We performed several tests to see how the walls would behave when heated up, how much heat the walls would withstand, and how much heat the walls would withstand when the heat input is high. The MPCMS performed better by reducing the wall temperature by 2.5-2.9°C, the thermal resistance loop by 6.3%, and the CHF by 7.7%. The constant melting and solidifying of the microcapsule contents made them more thermally stable and prevented the boiling fluctuations inside the loop from occurring [32].

Ritthong et al. (2024) Investigated a closed loop thermosyphon with three different diameters of copper tubes and three orientations of installations with the help of natural and forced convection techniques. The forced convection used was by an external fan fixed at 10.5 m/s. The range of inlet temperatures varied from 50-90°C for filled and unfilled conditions of the thermosyphon with refrigerant R410a to determine the effect of fluid charge, tube diameter, and orientation. A CFD model was created using ANSYS Fluent 2022 software to verify the thermal performance and heat transfer of the thermosyphon. The best performance was achieved by the 19.05 mm diameter filled tube with convection that is forced, which resulted in a power output of 1485 W, making it the most efficient [33].

3. HEAT PIPE LIMITATION

The efficiency of elevated the heat pipe's heat transmission is nevertheless restricted by the inherent limitations of heat pipes. limits, as shown in Figure (7), vicious limit, sonic, capillary, entrainment and boiling limit, are all phenomena within the heat pipe that decreases the power transfer efficiency of the heat pipe. The limits are contingent upon the selection of capillary structure, working substance, material, operating temperatures, and dimensions is critical. The heat pipes operation is primarily influenced by the delivered heat input, which determines the mass flow of the material being worked on within the pipe.

A- Viscous limit is reached under conditions of very low operating temperature and minimal applied heat load. So, this scenario, forces of viscosity prevail over the change in pressure, rendering the pressure gradient incapable of generating vapor flow. This is also referred to as a not-flow state. It is stated as,

$$Q_V = d_v^2 \, \lambda A_V \{ \frac{P_V \, \rho_V}{4(f_v R_{eV}) L_e \mu_V} \} \quad (1)$$

B- Sonic limit typically arises in heat pipes containing liquid metal. The initiation at low operating temperatures of the heat pipe is observable. This limit is shown by the equation below:

$$Q_S = A_v \rho_v \lambda \left[\left\{ \frac{\gamma v R_v Tv}{2(\gamma_v + 1)} \right\} \right]^{\frac{1}{2}} \quad (2)$$

C- Capillary limit is reached when the capillarity of pressures at the vapor-liquid contact in the evaporator and condenser are inadequate to overcome the frictional

pressure deficits associated with fluid motion. The maximum capillary pressure drop that a heat pipe can handle while it is running should be greater than the sum of all other pressure dips in the heat pipe, including the decrease in pressure caused by the vapor phase, the liquid phase, and gravity as shown in Equation (3).

$$\Delta P\ cp > \Delta P\ l + \Delta P\ v + \Delta P\ g \quad (3)$$

D- Entrainment limit is reached when the movement of mass of vapor is sufficient to displace liquid droplets that come from the outside of the capillary structure, resulting in the dryness of both the evaporator and the principal capillary structure.

It is articulated as,

$$Q_{Ent} = A_v \lambda \left[\frac{\sigma \rho_v}{2 r_h}\right]^{\frac{1}{2}} \quad (4)$$

E- Boiling limit is reached at elevated thermal fluxes. At this level, boiling bubble takes place within the main structure of the capillaries, leading to dryness of the main capillary structure. It also relies on how different the temperature is between the wall of the heat pipe and the working medium. It is given by Equation (5) [34] [15] [35] [36].

$$Q_{Bo} = 2\pi \frac{L_{ef} k_{e_f} Tv}{A_v \lambda \rho_v \ln\left(\frac{r_i}{r_v}\right)} \left[\frac{2\sigma}{r_n} - \Delta p_{Cmax}\right] \quad (5)$$

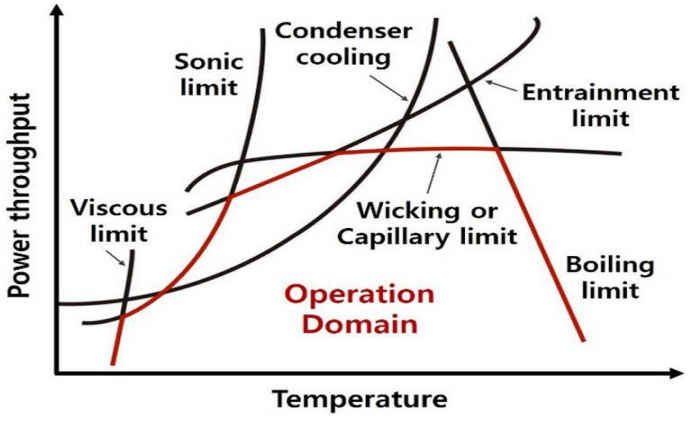

Fig. 7. Limits of heat pipes[37].

4. THERMOSYPHON

A thermosyphon is a device that is created by the buoyant forces that result from the gradient of density created by the temperature differences in the loop's heating and cooling components. Low heat resistance and the ability to function without a circulation pump are the thermosyphon's primary benefits[38].Heat pipe thermosyphons are classified into single-phase or two-phase loop thermosyphons and conventional thermosyphons[39]. Heat pipes and thermosyphons are effective devices for transferring heat passively that operate based on phase-change mechanisms. Among them, the loop thermosyphon offers better circulation and higher heat transport capability. Many recent studies have focused on improving their design and thermal performance under different conditions [40] [41].

Several parameters significantly influence the thermal performance of the loop thermosyphon whose schematics are shown in figure (8) [42]. The main influencing factors are summarized as follows:

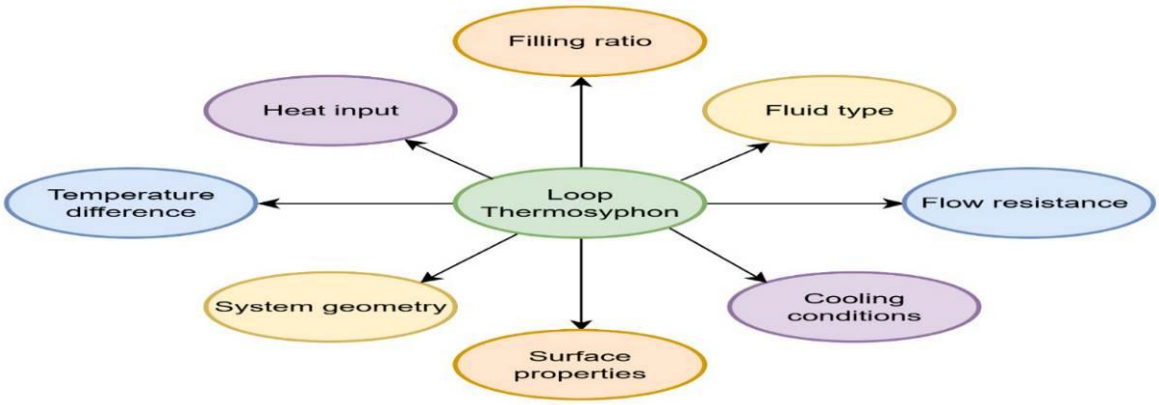

Fig. 8. Factors affecting the performance of the loop thermosyphon[42].

4.1. WORKING FLUID

A working fluid is a fluid within a closed system that enables its operation, including heating, cooling, or energy generation. The primary factor in the selection of a working fluid is the range of operating temperatures for vapor. The fundamental features required for a working fluid include compatibility with thermosyphon materials and geometries, as well as boiling point, thermal conductivity, low vapor and liquid viscosities and densities, latent heat, and surface tension. The choice of working fluid depends on the temperature at which the thermosyphon works. Another element influencing the picking of a working fluid is the consistency between the heat exchanger material and the fluid, specifically regarding low corrosion. The working fluid must be readily accessible, economically viable, and possess excellent thermal transfer characteristics, including high latent heat and high specific heat [43] .

Table 1. Different type of Working fluid [19]

NO	MEDIUM	MELTING POINT (°C)	BOILING POINT (°C)	USEFUL RANGE (°C)
1	HELIUM	-271	-261	-271 to -261
2	NITROGEN	-210	-196	-203 to -160
3	AMMONIA	-78	-33	-60 to 100
4	ACETONE	-95	57	0 to 120
5	METHANOL	-98	64	10 to 130
6	WATER	0	100	30 to 200
7	MERCURY	-39	361	250 to 650
8	SILVER	960	2212	1800 to 2300

Huang et al. (2021) Investigated a stainless-steel VCT, 262 mm long and charged with 3 ml methanol and 4.86 mg argon, heating the evaporator up to 400 W to examine its thermal response—this type of device is commonly used in thermal control for space systems. Using nine thermocouples along the adiabatic and condenser sections, the authors tracked wall-temperature variations and the shifting vapor–NCG interface. A 2D CFD model based on mass, momentum, energy, and species transport was developed to simulate the internal behaviour. The numerical predictions showed strong agreement with the experimental data, with an error of about 3–3.5%, confirming the reliability of the model [44].

4.2. FILLING RATIO (FR%)

The filling ratio is defined as a ratio of the volume of liquid to the total interior volume of the heat pipe [45]. The charge of the filling ratio will influence start-up performance, heat transfer efficiency, and isothermal performance. A lowered charge ratio of the working fluid will prolong the pressure accumulation process and result in the failure of heat pipe initiation. The evaporator tends to overheat with a low charge ratio, resulting in prolonged start-up times and a significant temperature differential within the heat pipe with elevated charge ratios. The heat pipe can only initiate and operate efficiently with an appropriate charge ratio [46].

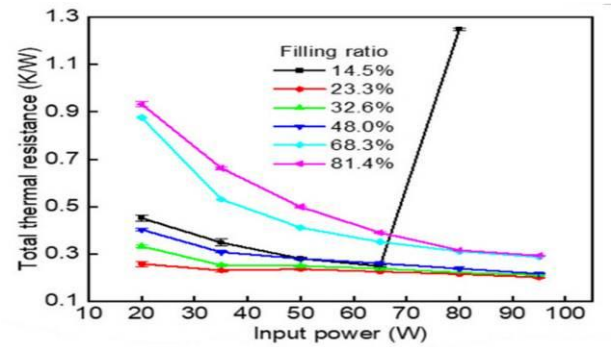

Fig. 9. The impact of filling rate and input power on overall thermal resistance [47].

T. Z. Farge et al. (2021) carried out an experimental study on a copper thermosyphon (26 mm OD, 24 mm ID) including only evaporator and condenser parts, devoid of an adiabatic part, with the evaporator submerged in transformer oil maintained at temperatures below 85°C. The distilled water was the operating fluid, and the filling ratios were 50%, 60%, and 70% at 100, 200, and 300 W of heat input. At 60% FR and 300 W, the highest performance was seen, with thermal resistance dropping by 14.6% compared to 50%. At 100 W, FR = 50% was more efficient, and the system started working at about 40°C. Increasing the power always lowered thermal resistance and improved cooling performance [48].

Wang et al. (2022) executed visual experimental research on (TPLT) constructed from transparent quartz glass (6 mm ID, 8 mm OD, 200 mm height) filled with N-pentane at 30–70% filling ratios. The evaporator (40 mm) was placed in a heated oil bath at 20 and 40 W, and the condenser (140 mm) was placed in a water-cooling jacket where water flowed at 23 ± 2 °C and 400 ± 20 g/min. This kept the condensation conditions stable. Experiments were done using vertical vibration of 30 m/s² and 35 Hz. They showed that vibration sped up the breaking of the liquid plug and changed the flow from plug to annular/wavy patterns. This made it easier to start up and made the flow more stable. At a filling ratio of 50% and an input power of 40 W, the best performance was seen [49].

Liu et al. (2025) Experimentally studied a two-phase loop thermosyphon with a comparison of a smooth tube condenser with a bellows-type condenser. A water-based thermosyphon system was developed with a range of filling ratios from 40% to 80%. A copper evaporator with a heat block and a transparent PTFE part was incorporated for the visualization of the flow. A condenser was placed inside a cooling water jacket with a 50-mm inner diameter. Water at a constant temperature of 18°C flowed at a rate of 0.017 L/s. Such a setup facilitated constant operation conditions for all the tests. A bellows tube was incorporated to enhance the condensation process by increasing the heat transfer area. For low filling ratios, the dry-out time was delayed, increasing the CHF from 359 to 399 W/cm². For high filling ratios, the thermal resistance was decreased by 13–18%. The thermal performance of the thermosyphon was better for the bellows condenser under various heat loads [50].

4.3. TYPES OF THERMOSYPHON

Compared to heat pipes, thermosyphons have a number of advantages. They are inexpensive to produce and maintain because of their straightforward structure and design. Thermosyphons can transfer heat over greater distances than heat pipes because they are not constrained by capillary action. Therefore, thermosyphons perform exceptionally well in gravity-assisted systems, which use gravity-driven natural circulation to enhance heat transmission. Operating at lower pressures makes component design simpler and lowers the chance of leaks [1].

A-conventional Two Phase Closed Thermosyphon (TPCT): whose schematics are shown in figure (12-a), A TPCT is a very effective heat transmitter that uses a liquid-vapor phase change. The heat absorbed causes the liquid to evaporate at the evaporator section. After passing through an adiabatic zone, the vapor condenses in the condenser, releasing heat into comparatively cold media. The liquid uses gravity to its advantage and returns to the evaporator in a thin layer of liquid film resembling a Nusselt. The evaporator, which involves a pool of liquid, is essentially positioned at the base of the TPCT [51].

Czerwiński and Wołoszyn, (2021) performed a numerical analysis of a cooling system utilizing phase change within a closed thermosyphon, modelled in ANSYS Fluent. A two-dimensional model was

utilized to simulate heat transfer and phase transition between liquid and vapor, while Lee's evaporation–condensation model was adjusted by incorporating variable mass-transfer relaxation parameters (re, rc) to improve numerical precision. The research determined that the best value of re = 1 s^{-1}, with rc varying according to phase densities, produced results that aligned with previously published data and showcased the model's efficacy in properly forecasting thermosyphon thermal performance [52].

Dimbarre et al. (2022) performed a numerical study utilizing ANSYS Fluent to examine the turbulent flow characteristics within the cooling jacket of a stainless-steel thermosyphon condenser. Their research concentrated on forecasting velocity distribution and pinpointing recirculation zones that influence cooling efficiency. The Reynolds Stress Model (RSM) was used to find the flow's turbulence characteristics, which showed that the flow is completely turbulent. The results showed that changing the geometry and flow direction makes convective heat transfer in the condenser portion better [53].

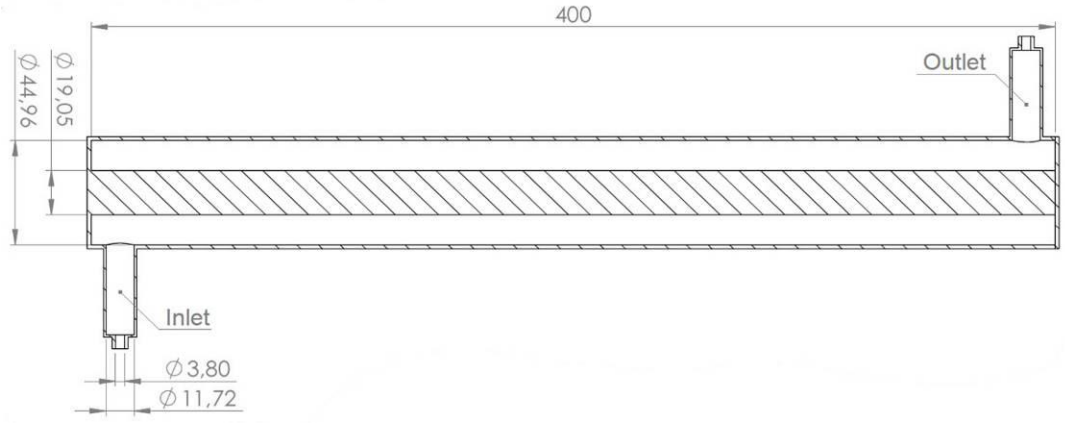

Fig. 10. Geometry of the cooling jacket used in the numerical simulation[53].

B- Two-Phase Loop Thermosyphon (TPLT): Loop thermosyphons are among the most widely used devices in the field of two-phase heat transfer because of their inexpensive cost, extended service life, excellent structural adaptability, and straightforward production procedure. Its gravity-assisted cycle uses no energy at all and has a sufficient temperature differential. The components of a loop thermosyphon include the internal two-phase working fluid, evaporator section, vapor line, condenser section, and liquid line which was shown in figure (12-b). The condenser section is often located at the top. The vapor line creates a closed-loop structure by joining the evaporator section's outlet and the condenser section's inlet, while the liquid line joins the condenser section's outlet and the evaporator section's input. A proper temperature differential between the evaporator and condenser portions is necessary for the internal working fluid to automatically create two-phase flow and heat transfer in a gravitational field. The natural flow state of the working fluid in TPLT is as follows: the liquid working fluid first absorbs heat from the evaporator's heat source and vaporizes, then the resulting vapor travels upward via the vapor line to the condenser section; it then releases heat to the condenser section's heat sink and condenses; and lastly, it travels downward via the liquid line to the evaporator section, completing a two-phase flow cycle [42] .

Remella and Gerner, (2023) performed a numerical and theoretical analysis of two-phase disjoined liquid–vapor flow within a small-channel with mesh walls in a closed-loop two-phase wicked thermosyphon (CLTPWT) utilized for the cooling of high-power LED modules. The research utilized ANSYS Fluent and Steady-State Thermal coupling to forecast temperature distribution, pressure reduction, and interfacial shear stress. The results showed that pressure and shear go up when heat is added, and flow reverses at 206 W, which is the operating limit. The research provides valuable insights into thermal fluid coupling for advanced

ATU- FJIMSE, Vol. 4 No. 1 (2026): volume 4,Issu 1,May 2026 , All Rights Reserved

electronic cooling systems. The schematic representation of the (CLTPWT) cooling system, which is applicable for high-power LED cooling, is shown in Fig (11) [54].

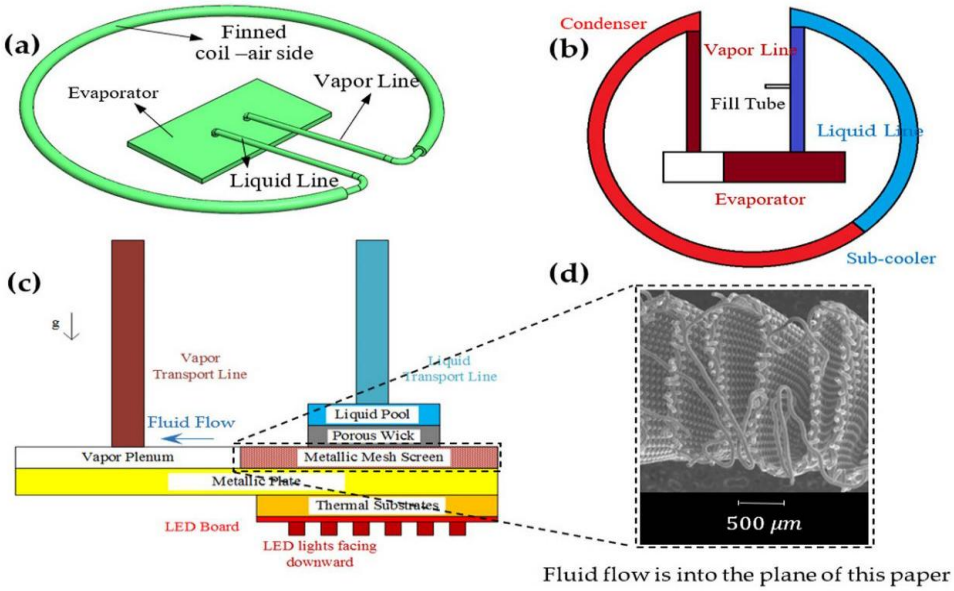

Fig. 11. (a) (CLTPWT), (b) different parts of the CLTPWT, (c) A side view of the evaporator package in 2D, and (d) E-SEM picture of the mesh screen channels [54].

Fuso et al. (2023) has conducted a thorough experimental study to investigate the thermal characteristics of a thermosyphon arrangement consisting of two loop thermosiphon systems, which were placed in parallel and series to be used as a hybrid solar system. A solar evaporator consisting of three vertical copper tubes and a backup evaporator were used. Distilled water was used as the working fluid, with a filling ratio of 100% for the solar evaporator and a range of 65 to 100% for the backup evaporator. The study focused on the temperature distribution and thermal resistance of the system under steady-state and fluctuating heat input, as well as simulating the occurrence of solar intermittence. Condensation occurred inside a main condenser equipped with a high-efficiency water jacket, which contained five internal baffles to improve heat transfer. This design considerably reduced the condensation resistance. The results showed that the parallel setup had lower overall thermal resistance and responded faster when the backup evaporator was turned on. On the other hand, the series configuration had better thermal performance consistency during the full day of operation [55].

Caner et al. (2024) the Open FOAM was used to numerically simulate a two-phase loop thermosyphon to generate a precise phase-change model. A hybrid model of the Tanasawa-Lee model was used for this purpose, using a methanol fluid with a 50% fill ratio and a heat input of 230 W. The numerical results showed that bubbles were formed and slug/plug flow was achieved with a thermal resistance of 0.26 K/W. This proved that the model was accurate enough to forecast TPLT thermal performance [56].

Le and Kim, (2025) conducted an extensive theoretical investigation of a two-phase loop thermosyphon, focusing on the analysis of boiling and condensation phenomena in the passive cooling systems of nuclear power plants. The research utilized computational fluid dynamics (CFD) as a theoretical framework to resolve the governing equations pertaining to heat and mass transfer within the loop. RPI Wall Boiling Model was used for the evaporator section of the loop, and a Wall Film Condensation Model was

ATU- FJIMSE, Vol. 4 No. 1 (2026): volume 4,Issu 1,May 2026 , All Rights Reserved

applied for the condenser section of the loop, all of which were implemented using UDFs within the ANSYS Fluent platform to provide a unified theoretical basis. Non-condensable gases were ignored. The outcomes provide a deeper insight into the heat transfer processes of loop thermosyphon systems and emphasize their potential for being applied in nuclear passive cooling technologies [57].

Jiang et al. (2025) proposed a novel asymmetric loop thermosyphon to improve the cooling capacity of rotating grinding wheels. At the theoretical level, the authors looked in to performance of the novel loop thermosyphon by using analytical expressions of thermal resistance, temperature uniformity, and Bond number to describe the effects of centrifugal forces and diameter change on the two-phase flow loop. At the experimental level, the copper loop, which had two inner diameters of 3 and 2 mm, was filled with acetone at a 50% filling ratio, and the evaporator was heated by a Ni–Cr wire, while the condenser was cooled by 0°C air from vortex tubes surrounding it. Tests up to 165 g showed that the asymmetric design reduced thermal resistance by about 44% and improved temperature uniformity compared with the symmetric loop [58].

C- Single Phase Loop Thermosyphon (SPLT): As shown in figure (12-c), Systems of natural circulation rely solely on convective flow caused by density gradients as a result of buoyancy-driven force; they are not dependent on any active power sources. Examples of natural circulation systems that are frequently used in engineering are single-phase thermosiphon loops. Thermosiphons, which are the prototype of passive safety devices, have garnered more attention in nuclear engineering, particularly for Gen 3+ and Gen 4 reactors. Nevertheless, temperature, pressure, and velocity field oscillations can impact thermosiphons and jeopardize their performance. Therefore, it is necessary to thoroughly examine the stability dynamics of single-phase free convection in order to improve the proper operation of thermosiphons. Natural circulation in single phases: A known collection of instabilities that arise for a specific combination of the operational parameters defines thermosiphon loops [59].

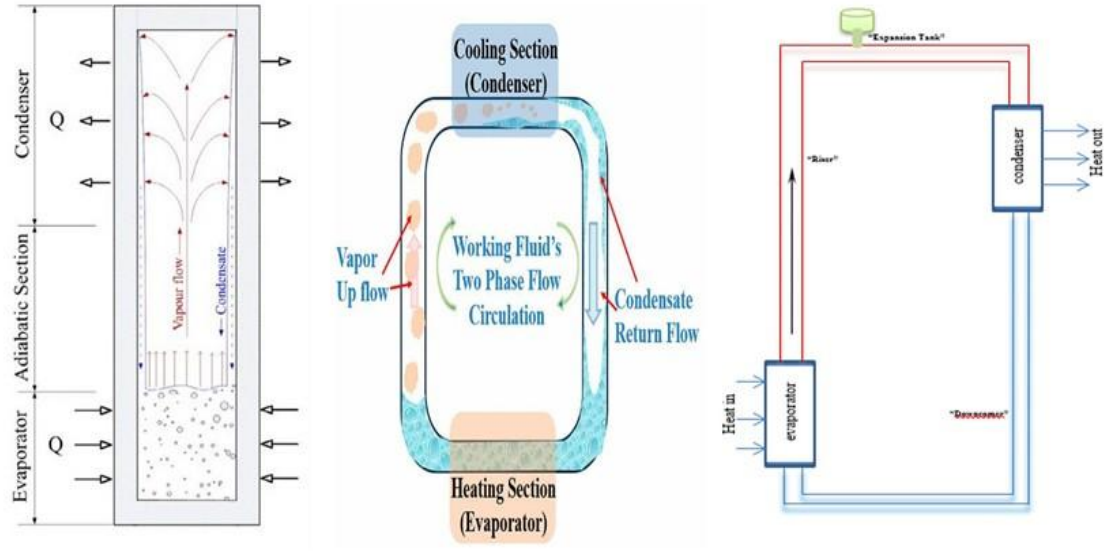

(a) **(b)** **(c)**

Fig. 12. Types of thermosyphon: (a) TPCT [60] , (b) TPLT [61] , and (c) SPLT [39].

5. GOVERNING EQUATIONS OF PHASE CHANGE FLOW

The calculation of the heat and mass transfer at the interface of the two-phase region can be accomplished by using the governing equations, which include the loading source term. The governing equations, which include the continuity, momentum, and energy equations, can be obtained by using Eqs (6), (12), and (17), respectively.

A- The continuity equation for the liquid and vapor phases

$$(\alpha_l / v\rho_l / v) + \nabla \cdot \left(\alpha_l / v\rho_l / v\,\vec{V}\right) = S_M \qquad (6)$$

α is the volume fraction, ρ is the density (kg/m^3), and V → is the fluid's velocity vector. The letters l and v stand for liquid and vapor, respectively. α is always in the range of 0 and 1 and $\alpha_v + \alpha_l = 1$. Consequently, the mass transfer source terms at the vapor/liquid interface are crucial for the accuracy and reliability of CFD simulations. Furthermore, based on its operational principle, the TPLT is propelled by the density differential between liquid and vapor, causing a change in pressure inside the loop.

A model of phase change depending on pressure:
superheat of the wall at the heating surface (αl = 1):

$$S_{M(l\to v)} = -S_{M(v\to l)} = \begin{cases} \beta_e \alpha_l \sqrt{\rho_v}\ \frac{P_{sat}(T)-P}{\sqrt{P}} & , \quad P_{sat}(T) \geq P+\Delta P_1 \\ 0 & , \quad P_{sat}(T) < P+\Delta P_1 \end{cases} \qquad (7)$$

contact between the liquid and vapor phases (0< αl<1):

$$S_{M(l\to v)} = -s_{M(v\to l)} = \beta_e \alpha_1 \sqrt{\rho_v}\ \frac{P_{Sat}(T)-P}{\sqrt{p}};\ \text{For evaporation, i.e .}\ P_{Sat}(T) \geq P \qquad (8)$$

$$S_{M(v\to l)} = -s_{M(l\to v)} = \beta_c \alpha_1 \sqrt{\rho_v}\ \frac{P_{Sat}(T)-P}{\sqrt{p}};\ \text{For evaporation, i.e .}\ P_{Sat}(T) < P \qquad (9)$$

βe and βc are the mass transfer frequencies of evaporation and condensation, in s^{-1}, respectively. Δp_i is the pressure potential difference required for the expansion of trapped gas or vapor in pits or cavities on the heating surface.

$$\Delta p_i = \frac{2\sigma_{lv}}{r_i}\left(1 + \frac{\rho_v}{\rho_l}\right) \qquad (10)$$

where σ_{lv} denotes surface tension in N/m, and ρ_v and ρ_l represent the densities of vapor and liquid, respectively, in kg/m^3. Meanwhile, ri denotes the radius of the vaporization core. Furthermore, $P_{Sat}(T)$ denotes the local saturation pressure associated with the local temperature, and its formulation is derived by fitting an equation with a maximum deviation of 0.1%.

$$p_{sat}(T) = e^{21.26955 - \frac{2775.456}{T-44.3757}} \quad (11)$$

(2) Momentum equation

$$\frac{\partial}{\partial t}(\rho\vec{v}) + \nabla \cdot (\rho\vec{v}\vec{v}) = -\nabla_p + \nabla[u((\nabla\vec{v} + \nabla\vec{v})^T)] + \rho g + F_{CSF} \quad (12)$$

The density and viscosity, ρ_{1v} and μ_{1v}, are described as the volume-averaged values of the mixed phase.

$$\rho = \alpha_l\rho_l + \alpha_v\rho_v \quad (13)$$
$$\mu = \alpha_l\mu_l + \alpha_v\mu_v \quad (14)$$

Furthermore, the continuum surface force F_{CSF} is applied to the momentum source term according to the model of continuum surfaces, which is derived as follows:

$$F_{csF} = 2\sigma_{lv}\ \frac{\alpha_l\rho_l C_v\nabla\alpha_v + \alpha_v\rho_v C_l\nabla\alpha_l}{\rho_l+\rho_v} \quad (15)$$

C denotes the curvature of the interface. σ_{1v} represents the surface tension in N/m, defined as:

$$\sigma_{lv} = -1.333 * 10^{-4} * T + 0.06275 \quad (16)$$

(3) Energy equation

$$\frac{\partial}{\partial t}(\rho E) + \nabla \cdot [(\rho E + p)\,\vec{v}] = \nabla \cdot (K\nabla T) + S_E \quad (17)$$

E energy is a value of mass-average:

$$E = \frac{\alpha_l\rho_l E_l + \alpha_v\rho_v E_v}{\alpha_l\rho_l + \alpha_v\rho_v} \quad (18)$$

"And the energy transfer source term" The formula for S_E is the mass source term S_M x the latent heat of vaporization λ.

$$S_E = \lambda * S_M \quad (19)$$

the expression for the latent heat of vaporization, denoted as λ, is:

$$\lambda = -8.758 * 10^{-3} * T^3 + 6.781 * T^2 - 2720 * T + 974300 \quad (20)$$

where the value of the volume fractions of liquid and vapor is also used to compute the thermal conductivity k_{lv} of the mixed phase.

$$k_{lv} = \alpha_l k_l + \alpha_v (n \times k_v) \quad (21)$$

where n is the thermal conductivity amplification factor [47]

6. APPLICATIONS OF HEAT PIPE THERMOSYPHON

geothermal energy extraction, solar collectors [62], turbine cooling[63], heat exchangers for waste heat recovery[64], electronics for high-performance thermal management[65], water heaters [66], Power generation[67] , air conditioning systems etc [68]. are just a few of the uses for thermosyphon applications. There are numerous uses for thermosyphon, which fall into the following four categories:

A-Applications for heat transfer, such as heat recovery and HVAC systems, where thermosyphon are employed as heat exchangers to transfer heat at a high rate.

B-Isothermal applications: In an isothermal furnace, thermosyphon are used to remove existing temperature gradients.

C-Electronics cooling systems: these employ thermosyphon to control the temperature of the electronic devices.

D-Transformation of heat flux applications: thermosyphon are employed in

circuit breakers and solar desalination plants, among other applications that need variable heat fluxes at the heat source and sink.

There is a particular temperature range in which the heat pipe operates for each application. Thus, the thermosyphon design should be focused on the desired temperature limits by using the appropriate working fluids [39].

7. CONCLUSIONS

The above review provided a structured overview of the heat pipe and thermosyphon technologies, with special emphasis placed on the improving of thermal performance, operational limits, and the behaviour of the two-phase systems, as discussed in the recent literature. It should be noted that the reviewed literature indicates the significance of the system's configuration and operational limits on the overall performance, as well as the enhancement techniques. In addition, the reviewed applications emphasize the increasing importance of thermosyphon systems in modern thermal management and energy-related fields. As a result of the insights obtained from the review, the proposed research work will be focused on the loop thermosyphon system using the theoretical and experimental approaches, with special emphasis placed on the enhancement of the condenser performance using the annular fin configurations.

REFERENCES

[1] Viveks Kumar, "ViveksThesis," Sep. 2023, doi: 10.7939/r3-zntw-mn29.
[2] M. Soliman, M. Shedid, H. A. El-Hameed, and H. Abou-Ziyan, "Effect of the State-of-the-Art Condenser Configuration on the Performance of Axially Rotating Wickless Heat Pipes," J Therm Sci Eng Appl, vol. 16, no. 9, Sep. 2024, doi: 10.1115/1.4065565.
[3] L. Perego Mendes et al., "Evaluation of Copper Diffusion Bonding Parameters Applied to the Manufacture of Flat Heat Pipes," Materials Research, vol. 28, 2025, doi: 10.1590/1980-5373-MR-2025-0065.
[4] A. Obaid and W. S. Sarsam, "Parametric Study of a Two-Phase Closed Thermosyphon Loop," Journal of Engineering, vol. 28, no. 5, pp. 92–118, May 2022, doi: 10.31026/j.eng.2022.05.06.
[5] D. Gamboa and B. Herrera, "Influence of Turbulence, Density, Phase Change, and Phase Interfaces Models on the Performance of the Numerical Simulation of a Two-Phase Closed Thermosyphon," TecnoLógicas, vol. 23, no. 49, pp. 53–70, Sep. 2020, doi: 10.22430/22565337.1563.
[6] R. Zhang and Z. Zhou, "Research and optimization of heat transfer characteristics of heat pipe-coupled phase change energy storage system," in Journal of Physics: Conference Series, Institute of Physics, 2024. doi: 10.1088/1742-6596/2838/1/012032.
[7] F. Celik and I. C. Bang, "Numerical Investigation of Filling Ratio Effects on Heat Pipe Performance: Modified Conduction Model."
[8] A. A. Bhatt, R. N. Patel, S. V. Jain, and D. V. Vaghela, "Experimental investigations on novel orientation study on axially grooved heat pipe with two evaporators and one condenser with multiple branches," Heat and Mass Transfer/Waerme- und Stoffuebertragung, vol. 60, no. 2, pp. 377–393, Feb. 2024, doi: 10.1007/s00231-023-03441-0.
[9] W. Zhou et al., "An Experimental Study of a Composite Wick Structure for Ultra-Thin Flattened Heat Pipes," Micromachines (Basel), vol. 15, no. 6, Jun. 2024, doi: 10.3390/mi15060764.
[10] S. Saadatian and H. Wong, "An analytic linear relation between the imposed heat flux and the pipe-end temperature for flat heat pipes with porous wicks," Int J Heat Mass Transf, vol. 245, Aug. 2025, doi: 10.1016/j.ijheatmasstransfer.2025.126950.
[11] Z. A. Faisal, A. A. Eidan, and A. Al-Manea, "Review of the effectiveness of heat pipe heat exchangers for waste heat recovery in HVAC systems," Sep. 30, 2025, Institute of Physics. doi: 10.1088/2631-8695/ae05e7.
[12] N. A. Moayad and W. S. Sarsam, "Theoretical and Experimental Investigation of an Acetone-Filled Pulsating Heat Pipe Heat Exchanger for Waste Heat Recovery," Journal of Engineering, vol. 31, no. 9, pp. 191–207, Sep. 2025, doi: 10.31026/j.eng.2025.09.12.
[13] M. A. Yassin, H. M. Abd El-Hameed, M. H. Shedid, and H. Abou-Ziyan, "Effect of Operating Parameters on the Performance of Axially Rotating Horizontal Heat Pipe: Experimental Investigation," Engineering Research Journal, vol. 182, no. 2, pp. 257–287, Jun. 2024, doi: 10.21608/erj.2024.358706.
[14] Y. Xiang et al., "Study on Heat and Mass Transfer Performance of Ultra-Thin Micro-Heat Pipes," Energies (Basel), vol. 17, no. 14, Jul. 2024, doi: 10.3390/en17143426.
[15] M. Malcho, J. Jandačka, R. Lenhard, K. Kaduchová, and P. Nemec, "Applications of Heat Pipes in Thermal Management," Energies (Basel), vol. 18, no. 19, p. 5282, Oct. 2025, doi: 10.3390/en18195282.
[16] J. K. Abdali and A. A. Alwan, "Theoretical Model to Investigate the Heat Transfer Mechanism through a Heat Pipe with Graphene Oxide/Distilled Water as Working Fluid," in IOP Conference Series: Materials Science and Engineering, IOP Publishing Ltd, Nov. 2020. doi: 10.1088/1757-899X/987/1/012017.

ATU- FJIMSE, Vol. 4 No. 1 (2026): volume 4,Issu 1,May 2026 , All Rights Reserved

[17] P. Bhadra* and B. Ch. Nookaraju, "Experimental and Numerical Analysis of Composite Wick Heat Pipes using Ethanol," International Journal of Innovative Technology and Exploring Engineering, vol. 9, no. 3, pp. 2360–2363, Jan. 2020, doi: 10.35940/ijitee.C8882.019320.
[18] D. K. Jain and A. V Deshpande, "Mathematical Modelling and Optimization of Cylindrical Heat Pipe."
[19] J. KADHIM Abdali, A. Abbas Alwan, and R. H. Hameed, "Heat Pipe and Applications-Recent Advances and Review," May 2020. [Online]. Available: https://www.researchgate.net/publication/344442623
[20] S. U. Khalid, H. Babar, H. M. Ali, M. M. Janjua, and M. A. Ali, "Heat pipes: progress in thermal performance enhancement for microelectronics," J Therm Anal Calorim, vol. 143, no. 3, pp. 2227–2243, Feb. 2021, doi: 10.1007/s10973-020-09820-7.
[21] Y. Feng, X. Wu, C. Liang, and Z. Sun, "A Convenient Method for the Accurate Calculation of Fin Efficiency of H-Type Fins Based on Linear Nomograms and Fitting Formulae," Energies (Basel), vol. 15, no. 2, Jan. 2022, doi: 10.3390/en15020456.
[22] E. A. Hummood and M. Hasan, "Enhancing the performance of earth to air heat exchanger using annular and perforated fins ; numerical and experimental study," Feb. 16, 2024. doi: 10.21203/rs.3.rs-3943996/v1.
[23] M. A. Yassin, H. M. Abd El-Hameed, M. H. Shedid, and H. Abou-Ziyan, "Enhancing the Experimental Performance of Axially Rotating Wickless Heat Pipe Using Annular-and Longitudinally Finned Condensers," J Therm Sci Eng Appl, vol. 16, no. 11, Nov. 2024, doi: 10.1115/1.4066261.
[24] J. Singh et al., "Numerical Analysis of Laminar Flow and Heat Transfer in Micro Pin Fin Heat Sinks with Varying Fin Geometries: Effect of Fin Geometry on Micro Pin Fin Heat Sinks," Aug. 08, 2025. doi: 10.20944/preprints202508.0610.v1.
[25] P. Srinivas Kishore, K. V Siva Kumar, and P. S. Kishore, "Estimation of Heat Transfer with Helical Fins at Annulus in a Double Pipe Heat Exchanger," International Journal of Research and Analytical Reviews, 2023, [Online]. Available: https://www.researchgate.net/publication/374118253
[26] R. Saeidi, Y. Noorollahi, S. Chang, and H. Yousefi, "A comprehensive study of Fin-Assisted horizontal ground heat exchanger for enhancing the heat transfer performance," Energy Conversion and Management: X, vol. 18, Apr. 2023, doi: 10.1016/j.ecmx.2023.100359.
[27] Y. M. Seo, H. Y. Choi, R. K. Ko, S. Kim, and Y. G. Park, "Artificial Neural Network Modeling on Heat Transfer Performance of Finned Heat Pipe," May 22, 2024. doi: 10.21203/rs.3.rs-4361511/v1.
[28] D. Brough, J. Ramos, B. Delpech, and H. Jouhara, "Development and validation of a TRNSYS type to simulate heat pipe heat exchangers in transient applications of waste heat recovery," International Journal of Thermofluids, vol. 9, Feb. 2021, doi: 10.1016/j.ijft.2020.100056.
[29] Al-Amin, R. I. Reja, Md. A. A. Sumon, S. Alam, and M. Z. Abedin, "Performance Analysis of Annular Fins in Cylindrical Pipes: A Study on Heat Transfer and Fin Efficiency under Various Convection Modes," SciEn Conference Series: Engineering, vol. 3, pp. 281–285, Nov. 2025, doi: 10.38032/scse.2025.3.79.
[30] M. Ahmed, I. Rofaiel, and M. Essa, "Experimental study for the performance of an integrated solar collector water heater based on helical fins heat pipes using phase changing material," The Egyptian International Journal of Engineering Sciences and Technology, vol. 30, no. Mechanical Engineering, pp. 22–38, Aug. 2020, doi: 10.21608/eijest.2020.104931.
[31] S. Tawsif Islam, "Closed Loop Thermosyphon," 2023, doi: 10.13140/RG.2.2.28037.01762.

[32] Z. Tan, X. Li, J. Zhou, and X. Huai, "Experimental study on a loop thermosyphon with microencapsulated phase change material suspension," in Journal of Physics: Conference Series, Institute of Physics, 2024. doi: 10.1088/1742-6596/2707/1/012158.
[33] N. Ritthong, S. Thongkom, A. Sawisit, B. Duangsa, and W. Ritthong, "Optimization Design of Closed-Loop Thermosyphons: Experimentation and Computational Fluid Dynamics Modeling," Energies (Basel), vol. 17, no. 2, Jan. 2024, doi: 10.3390/en17020527.
[34] R. Caruana and M. Guilizzoni, "Modeling of Conventional Heat Pipes with Capillary Wicks: A Review," May 01, 2025, Multidisciplinary Digital Publishing Institute (MDPI). doi: 10.3390/en18092213.
[35] U. Singh and N. Kumar Gupta, "Operational Limitations of Heat Pipes with MgO-Water Nanofluid: An Experimental Investigation," IOP Conf Ser Mater Sci Eng, vol. 1116, no. 1, p. 012054, Apr. 2021, doi: 10.1088/1757-899x/1116/1/012054.
[36] D. M. Weragoda, G. Tian, A. Burkitbayev, K. H. Lo, and T. Zhang, "A comprehensive review on heat pipe based battery thermal management systems," Apr. 01, 2023, Elsevier Ltd. doi: 10.1016/j.applthermaleng.2023.120070.
[37] I. N. Jang and Y. S. Ahn, "Sintered Wick Heat Pipes with Excellent Heat Transfer Capabilities—Case Study," Energies (Basel), vol. 17, no. 5, Mar. 2024, doi: 10.3390/en17051113.
[38] A. A. A. Aljuboori, S. Y. Ahmed, and M. Y. Jabbar, "Experimental study of closed-loop thermosyphon with a different evaporator geometry," Heat Transfer, vol. 50, no. 1, pp. 466–486, Jan. 2021, doi: 10.1002/htj.21887.
[39] A. A. Abdulaziz, "Characteristics of Heat Transfer in Closed Loop Thermosyphon with Different Evaporator Geometry."
[40] A. Rukruang, H. Y. Lin, J. Kaew-On, and C. C. Wang, "Experimental investigation on thermal performance of multiport minichannel flattened tube thermosyphon heat exchanger," Appl Therm Eng, vol. 257, Dec. 2024, doi: 10.1016/j.applthermaleng.2024.124385.
[41] jihad .Kadhim .AbdAli .Abdullah and Adil Abbas Alwan Al-Moosawy, "Experimental and Numerical Investigation of Transient heat pipe," 2021.
[42] C. Chen et al., "Characterisation of a controllable loop thermosyphon for precise temperature management," Appl Therm Eng, vol. 185, Feb. 2021, doi: 10.1016/j.applthermaleng.2020.116444.
[43] A. Obaid and W. S. Sarsam, "Investigation of Thermal Performance of a Two-Phase Thermosyphon System Using Different Working Fluids," 2021.
[44] C. N. Huang, K. L. Lee, C. Tarau, Y. Kamotani, and C. R. Kharangate, "Computational fluid dynamics model for a variable conductance thermosyphon," Case Studies in Thermal Engineering, vol. 25, Jun. 2021, doi: 10.1016/j.csite.2021.100960.
[45] H. Zhang, H. Xu, and C. Tian, "Startup influencing factor investigation and quantitative interaction analysis on a loop thermosyphon with multiple evaporators," Case Studies in Thermal Engineering, vol. 28, Dec. 2021, doi: 10.1016/j.csite.2021.101460.
[46] H. Zhang, F. Ye, H. Guo, and X. Yan, "Isothermal Performance of Heat Pipes: A Review," Mar. 01, 2022, MDPI. doi: 10.3390/en15061992.
[47] H. Yao et al., "Characteristics of phase-change flow and heat transfer in loop thermosyphon: Three-dimension CFD modeling and experimentation," Case Studies in Thermal Engineering, vol. 35, Jul. 2022, doi: 10.1016/j.csite.2022.102070.
[48] T. Z. Farge, S. J. Ismael, and R. M.Thyab, "Experimental Investigation of Thermosyphon Thermal Performance Using Different Filling Ratio," Engineering and Technology Journal, vol. 39, no. 1A, pp. 34–44, Jan. 2021, doi: 10.30684/etj.v39i1a.1639.

[49] Z. Wang, F. Li, and M. Cha, "EXPERIMENTAL INVESTIGATION OF FLOW CHARACTERISTICS IN A VERTICAL VIBRATION TWO-PHASE LOOP THERMOSYPHON," Thermal Science, vol. 26, no. 5, pp. 4367–4376, 2022, doi: 10.2298/TSCI211023014W.
[50] Z. Liu, Y. Cai, J. Lu, Y. Li, D. Tang, and C. Hu, "The thermal performance of bellows tube as a condenser in two-phase loop thermosyphon within a wide range of filling ratios," International Communications in Heat and Mass Transfer, vol. 169, Dec. 2025, doi: 10.1016/j.icheatmasstransfer.2025.109566.
[51] Z. Lataoui, A. M. Benselama, and A. Jemni, "Heat Transfer Characteristics of Thermosyphons Used in Vacuum Water Heaters," Fluids, vol. 10, no. 8, Aug. 2025, doi: 10.3390/fluids10080199.
[52] G. Czerwiński and J. Wołoszyn, "Numerical study of a cooling system using phase change of a refrigerant in a thermosyphon," Energies (Basel), vol. 14, no. 12, Jun. 2021, doi: 10.3390/en14123634.
[53] V. Vaurek Dimbarre, F. Mercês Biglia, L. E. M. Lima, P. H. DIAS DOS SANTOS, and T. Antonini Alves, "Numerical analysis of the turbulent flow of the cooling jacket applied in a stainless steel thermosyphon," Associacao Brasileira de Engenharia e Ciencias Mecanicas - ABCM, Oct. 2022. doi: 10.26678/abcm.eptt2022.ept22-0022.
[54] K. S. Remella and F. M. Gerner, "Separated Liquid–Vapor Flow Analysis in a Mini-Channel with Mesh Walls in the Closed-Loop Two-Phase Wicked Thermosyphon (CLTPWT)," Energies (Basel), vol. 16, no. 13, Jul. 2023, doi: 10.3390/en16135045.
[55] L. Serconek Fuso, L. H. R. Cisterna, and M. B. H. Mantelli, "Experimental study of two phase loop thermosyphons for hybrid solar systems," Energy Convers Manag, vol. 293, Oct. 2023, doi: 10.1016/j.enconman.2023.117550.
[56] J. Caner, E. Videcoq, A. M. Benselama, and M. Girault, "Simulation of a two-phase loop thermosyphon using a new interface-resolved phase change model," Int J Heat Mass Transf, vol. 228, Aug. 2024, doi: 10.1016/j.ijheatmasstransfer.2024.125607.
[57] Q. T. Le and B. J. Kim, "CFD Simulation of Loop Thermosiphon Using the Wall Boiling and Condensation Models," in Proceedings of the World Congress on Momentum, Heat and Mass Transfer, Avestia Publishing, 2025. doi: 10.11159/icmfht25.105.
[58] F. Jiang, N. Qian, J. Chen, M. Bernagozzi, M. Marengo, and Y. Fu, "3D asymmetric loop thermosyphon under radial rotation: A novel method for enhanced heat transfer in grinding," International Journal of Thermal Sciences, vol. 219, Aug. 2025, doi: 10.1016/j.ijthermalsci.2025.110219.
[59] T. Nguyen Ken, M. Alice Lindquist, and E. Merzari Ken, "On the Impact of Aspect Ratio and Other Geometric Effects on the Stability of Rectangular Thermosiphons."
[60] B. A. ZAHRAA ABBAS FAISAL Supervised by Adel Eidan, "ENHANCING THERMAL PERFORMANCE OF HEAT PIPE HEAT EXCHANGER USING DIFFERENT TECHNIQUES NUMERICALLY AND EXPERIMENTALLY A THESIS SUBMITTED TO THE DEPARTMENT OF MECHANICAL ENGINEERING TECHNIQUES OF POWER IN PARTIAL FULFILLMENT OF THE REQUIREMENTS FOR PH.D. DEGREE IN MECHANICAL ENGINEERING-THERMAL," 2025.
[61] J. C. Jang, T. K. Lim, J. S. Lee, and S. H. Rhi, "Li-Ion Battery Cooling and Heating System with Loop Thermosyphon for Electric Vehicles," Energies (Basel), vol. 18, no. 14, Jul. 2025, doi: 10.3390/en18143687.
[62] M. M. Soliman, M. H. Shedid, H. M. Abd El-Hameed, and H. Abou-Ziyan, "EXPERIMENTAL INVESTIGATION OF THE EFFECT OF CONDENSER CONFIGURATION ON A HORIZONTALLY ROTATING WICKLESS HEAT PIPE PERFORMANCE," 2025. [Online]. Available: www.begellhouse.com

[63] M. Polačiková, P. Nemec, M. Malcho, and J. Jandačka, "Experimental Investigations of a Passive Cooling System Based on the Gravity Loop Heat Pipe Principle for an Electrical Cabinet," Applied Sciences (Switzerland), vol. 12, no. 3, Feb. 2022, doi: 10.3390/app12031634.
[64] M. A. Hussain et al., "THERMAL PERFORMANCE OF SINTERED COPPER WICK HEAT PIPE USING WATER-BASED HYBRID NANOFLUIDS: AN EXPERIMENTAL STUDY," 2022. [Online]. Available: www.begellhouse.com
[65] F. N. Al-Mousawi, N. S. Dhaidan, A. A. Mohammed, A. A. Alammar, and R. Z. Homod, "Investigation of the performance of a heat pipe using various configurations and innovation designs: a review," J Therm Anal Calorim, 2025, doi: 10.1007/s10973-025-14711-w.
[66] R. S. Anand, C. P. Jawahar, A. Brusly Solomon, S. David, E. Bellos, and Z. Said, "Experimental investigations on modified thermosyphons using R134a/Al2O3 and comparative machine learning analysis," Appl Therm Eng, vol. 212, Jul. 2022, doi: 10.1016/j.applthermaleng.2022.118554.
[67] V. K. Mishra, S. K. Panda, B. Sen, and D. Samantaray, "An Experimental Investigation on Heat Transfer Performance of a Thermosyphon With External Fins," Heat Transfer, 2025, doi: 10.1002/htj.70093.
[68] S. Y. Zakaria, A. G. Ibrahim, A. M. Rashad, and S. E. El-Shamarka, "Experimental investigation and numerical simulation of the thermosyphon heat pipe charged with R134a," in IOP Conference Series: Materials Science and Engineering, IOP Publishing Ltd, Nov. 2020. doi: 10.1088/1757-899X/973/1/012039.